Unusual optical observations of OI greenline during a geospace event on 1 February 2008

V. Lakshmi Narayanan,[1] S. Gurubaran,[1] K. Emperumal,[1] and P. T. Patil[2]

Received 1 December 2010; revised 26 May 2011; accepted 28 June 2011; published 21 September 2011.

[1] We herein report the first observations of an unusual phenomenon recorded by an all-sky airglow imager from the low-latitude site Panhala (16.8°N, 74.1°E, geographic; 8.2°N geomagnetic), on the night of 1 February 2008, during the main phase of a moderate geomagnetic storm. The observations of OI 557.7 nm emission reveal discrete, transient, filamentary structures referred to as "streaks." No such features were seen in the OI 630.0 nm emission and the mesospheric sodium and hydroxyl emissions. Here we speculate on possible mechanisms for generation of such structures, though we cannot conclude firmly that any one of them was responsible for the observed features. This is a puzzling observation made from very low geomagnetic latitude during the main phase of a moderate recurrent geomagnetic storm in the declining phase of solar cycle. In spite of the limitations in identifying the mechanism or mechanisms responsible for this striking observation, it is felt that understanding of processes driving such unusual and rare events will substantiate our knowledge on the mysterious coupling processes occurring in the equatorial upper atmosphere.

Citation: Narayanan, V. L., S. Gurubaran, K. Emperumal, and P. T. Patil (2011), Unusual optical observations of OI greenline during a geospace event on 1 February 2008, *J. Geophys. Res.*, *116*, A09315, doi:10.1029/2010JA016339.

1. Introduction

[2] The distinction between auroral and airglow emissions lies in the fact that the former is caused by energetic charged particles while the latter gets excited by solar photons and exothermic chemical reactions. Auroral observations made at latitudes outside the auroral zone are generally referred to as low latitude aurorae. Historical records from several locations in the middle and low geomagnetic latitudes rarely contain evidences in support of the reports on the visual observation of such sporadic aurorae [*Chapman*, 1957; *Silverman*, 2003; *Willis et al.*, 2007]. With the advent of modern optical instrumentation, recording of faint emissions in the sub-visual threshold had become feasible and some observations have been made from mid and low latitudes [*Tinsley*, 1979; *Tinsley et al.*, 1984, 1986; *Shiokawa et al.*, 2005]. According to our knowledge, no structural features were reported in these low latitude auroral observations. On the other hand, for about a decade the studies of artificial generation of airglow by transmission of high power HF radio waves have been gaining importance [*Bernhardt et al.*, 1988; *Kagan et al.*, 2000; *Gurevich et al.*, 2002; *Mishin et al.*, 2004; *Pederson et al.*, 2008]. Since the mechanism of excitation is attributed to superthermal electrons in such cases, these artificially generated emissions are also referred to as artificial aurora [*Kagan et al.*, 2000, 2009].

[3] Herein, we report observations of puzzling structural features noticed only in OI 557.7 nm airglow during a moderate geomagnetic disturbance. The available particle precipitation data from POES satellites and ground station ionograms over geomagnetic equator reveal the occurrence of energetic neutral atom precipitation and existence of enhanced ionization at E region heights during the observation period. We speculate possible origins of these structures and propose natural radio wave heating of the E region ionosphere as a potential mechanism capable of generating these features. The main aim of this report is to bring this puzzling observation to the notice of scientific community, thereby motivating search for similar observations from other sites and discussion on the possible source of the event.

2. Observations and Inferences

[4] Routine all-sky imaging observations of prominent airglow emissions are being made from the magnetic equatorial station, Tirunelveli (8.7°N; 77.8°E; 0.17°S geomagnetic) from early 2007. A vertical incidence Canadian Advanced Digital Ionosonde is in regular operation at Tirunelveli from June 2006. Ionograms are usually collected at 15 min temporal spacing from this equatorial station. During January–March 2008, the all-sky imager was moved to Panhala and observations were made in campaign mode with the primary objective of studying the dynamics of the mesosphere-lower thermosphere (MLT) region and plasma depletions in the ionosphere. From early 2009, routine imaging observations are being made with similar imager from Kolhapur (17.0°N;

[1]Equatorial Geophysical Research Laboratory, Indian Institute of Geomagnetism, Tirunelveli, India.
[2]Radar Observatory, Indian Institute of Geomagnetism, Shivaji University Campus, Kolhapur, India.

0148-0227/11/2010JA016339

Table 1. Filter Characteristics, Exposure Times of Images, and Spatial Resolution at Emission Heights

Emission Wavelength (nm)	Assumed Centroid Height (km)	Filter Peak Transmission Wavelength (nm)	Filter Bandwidth (nm)	Peak Transmission (%)	Exposure Times (s)	Spatial Resolution at Emission Heights (km)	
						Horizontal	Diagonal
OI (630.0)	275	629.9	2.37	78.87	120	1.78	2.53
OI (557.7)	97	557.8	1.79	53.5	120	0.57	0.81
Na (589 and 589.6)	90	589.2	1.98	71	120	0.53	0.76
OH Meinel band	87	705.3–928.2 (notch ~865)	…	93.6	30	0.51	0.73
Background filter	…	572.3	1.95	84	120	…	…

74.0°E), a location situated at ~20 km distance from Panhala. Imagers of this kind were operated in the past from middle and low latitudes to study the atmospheric wave perturbations manifested in airglow intensities [e.g., *Taylor et al.*, 1995; *Narayanan et al.*, 2010], monitor the traveling ionospheric disturbances [e.g., *Shiokawa et al.*, 2002], plasma depletions [e.g., *Abalde et al.*, 2001] and low latitude auroral emissions during magnetic storms [*Shiokawa et al.*, 2005]. The observations reported in this study are unique in that the features described here were observed only on the night of 1 February 2008 and it is affirmed that the phenomenon observed is truly geophysical to the best of our knowledge.

[5] The current imager is designed for F/4 optics and is equipped with a fish eye lens at the front end followed by a telecentric lens pair. A six-position filter wheel holds the interference filters below the telecentric lens pair. The parallel beams from the telecentric lens pair pass through the interference filters and are reimaged into a CCD camera. Acquisition of images is made through a highly sensitive back illuminated CCD (512 × 512 array). The filter properties, exposure times given to obtain individual images and the respective spatial resolution at emission altitudes are given in Table 1. The acquired airglow images on any night were flat fielded and subtracted from an average of several star-removed images before projecting them into the geographical coordinate grid. The instrument details and the image processing techniques adopted in the present work are discussed by *Narayanan et al.* [2009, and references therein].

[6] Figure 1 shows a set of images obtained on the night of 1 February 2008 that are projected on the latitude-longitude grid. The region of the sky observed within a field of view of 130° is used for projection in order to restrict vehicular reflections from nearby road. These are processed images shown in false-color mode whose individual pixel values were not calibrated to absolute intensities. An intense region extending from northwest to southeast near the center of each of the images was caused by the Milky Way. The image acquisition times indicated in the panels are in UT (=LT-5.5 h).

[7] A striking feature of the OI 557.7 nm (green-line) images that was not present in sodium, hydroxyl and OI 630.0 nm (red-line) emissions was the presence of narrow, transient, streaks observed between 16:20 and 18:35 UT (pre-midnight sector in magnetic local time), with longer and long-lived (~10 min and above) streaks observed during the first hour of this period and shorter streaks with relatively smaller lifetimes observed during the rest of the period. The first streak was the longest one with a life time of about 16 min and two of the observed streaks had a shortest life time of ~2 min. From the sequence of OI 557.7 nm images, it was noticed that the streaks were aligned at an angle of ~13° to the west of the geomagnetic meridian (~15° to the west of geographic North) and drifted westward at speeds in the range of 30–50 m/s. Several streaks were seen to elongate from south to north along their length. Fresh streaks always formed to the east of the existing streaks. The lengths of individual streaks varied from several tens of kilometers to ~200 km, whereas their width was of a few km in the emitting region at ~100 km. The maximum width was ~10 km. Their drift velocities, lengths and widths were computed with an assumed emission altitude of 97 km for OI green line. The relative percentage brightness of the streaks was about 20–25% of the background OI 557.7 nm emission. At least 15 individual streaks were identified and a striking similarity between all the observed streaks during this period was their preference to be aligned at the same inclination to the geomagnetic meridian. The last streak disappeared at 18:35 UT (corresponding to local midnight).

[8] During this period, the Earth's magnetosphere was buffeted by a fast solar wind stream that emerged from a coronal hole on January 29, 2008. Such high speed streams are referred to as Corotating Interaction Regions (CIR) and they are associated with the 27-day recurrent geomagnetic activity. A moderate magnetic storm (with minimum quick-look Dst of −44 nT) occurred immediately after a southward turning of the interplanetary magnetic field (IMF) on 1 February 2008. In Figure 2a we show the x-component (directed toward Earth) of the solar wind velocity, and in Figures 2b and 2c we show the B_z and B_y components, respectively, of the IMF in GSM coordinates. The AU and AL indices (provisional values derived from nine stations) are shown for this day in Figure 2d. The B_z component of IMF turned southward at ~14:30 UT and experienced two short northward fluctuations during the next one hour, after which it remained southward till 18:00 UT. Prolonged southward IMF is known to cause enhanced magnetospheric convection leading to the main phase of a magnetic storm through injection of energetic charged particles into the inner magnetosphere in and around the equatorial plane. Now it is well known that fluxes of relativistic electrons in CIR driven storms are more severe than that in Coronal Mass Ejection (CME) driven storms [*Baker et al.*, 1987; *Borovsky and Denton*, 2006]. The growth and decay of the ensuing ring current can be easily identified in ground magnetic records from a low latitude site. In Figure 2e we have used the ground magnetic data representing the northward magnetic field perturbation (ΔH) obtained from the low latitude magnetometer station, Alibag (10.2°N, geomagnetic) in the Indian sector, to track the evolution of the ring current during the main phase of the ongoing magnetic storm. The

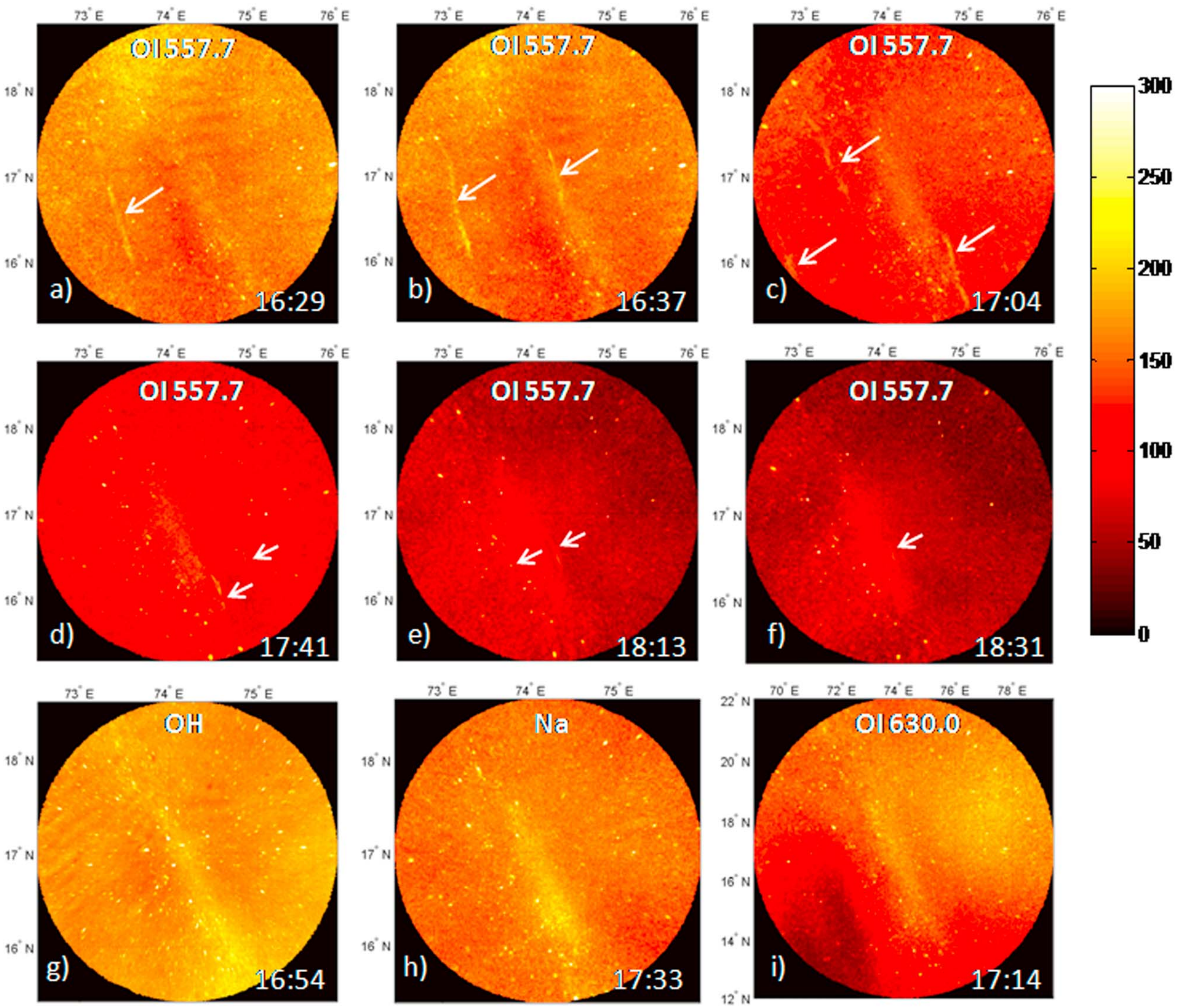

Figure 1. All-sky airglow images obtained from Panhala on 1 February 2008. Shown are (a–f) OI 557.7 nm, (g) OH Meinel bands, (h) Na 589.2 nm, and (i) OI 630 nm emissions. The images are given in false color mode.

auroral electrojet indices reveal the occurrence of a magnetospheric substorm, which is believed to be the result of an explosive release of energy stored in the geomagnetic tail when the IMF turns northward. It might seem probable that the onset of substorm that occurred around 17:00 UT also contributed to the injection of energetic particles into the inner magnetosphere to partly account for the growth of the ring current.

[9] Energetic electron and proton fluxes made use of in this work were measured by Medium Energy Proton and Electron Detector (MEPED) instruments onboard NOAA/Polar Orbiting Environmental Satellites (POES) (NOAA-15, 16, 17 and 18) and METOP-02 satellite that orbit at an altitude of about 850 km. The fluxes are measured separately at 0° and 90° corresponding to approximate vertical and horizontal directions, respectively. At low latitudes, the trapped and precipitating ions are expected to be measured by the 0° and 90° detectors, respectively. The vice versa applies to the high latitudes. Figure 3a shows the plot of particle flux measurements made by 90° detectors corresponding to magnetic shells with $L < 7$. Beginning at ~17:30 UT, the measured fluxes reveal enhanced energetic ions in the energy range 30–300 keV for electron fluxes and 30–240 keV for proton fluxes at L-values as low as ~4.5 as shown in Figure 3b. It was not possible to confirm the presence of these energetic particle fluxes for the first one hour of streak observations (16:20–17:20 UT), because the orbital passes of all the five satellites were well outside the midnight sector where the energization and injection of particles into the ring current are expected to occur. Hence, it is reasonable to expect that the particle precipitation commenced at an earlier time in concurrence with the occurrence of streaks in OI 557.7 nm emission reported herein.

[10] A notable manifestation of this storm in the equatorial F region was the rise of the F-layer height that began at around 16:30 UT. Figure 4 depicts the time-variation of the

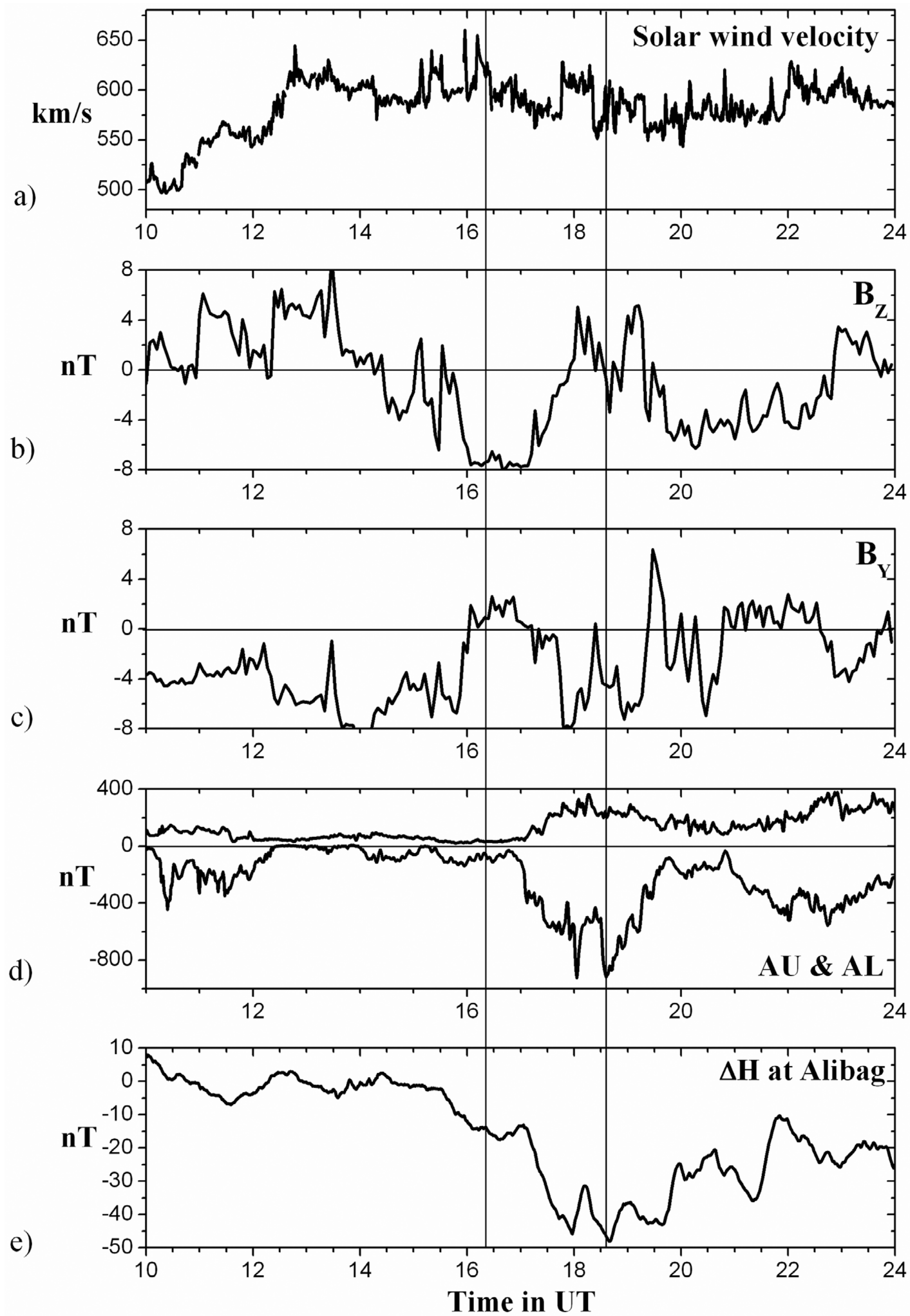

Figure 2. Interplanetary conditions and ground observations of the geospace event: (a) solar wind velocity, (b) z-component of interplanetary magnetic field (IMF) in GSM coordinates, the component along geomagnetic dipole axis, (c) y-component of IMF in GSM coordinates, the dawn-to-dusk component, (d) AU and AL indices (provisional values), and (e) ΔH at Alibag (10.2°N geomagnetic). The vertical lines through all plots indicate the time of observation of filamentary streaks.

height of the 3 MHz frequency as observed in the ground ionograms recorded at the magnetic dip equatorial station, Tirunelveli in the same longitude sector. Ionospheric effects during magnetospheric disturbances are known to arise from (1) prompt penetration of magnetospheric electric fields to equatorial latitudes and (2) delayed disturbance dynamo electric field arising from a perturbed thermospheric wind circulation driven by storm energy inputs at high latitudes [*Fejer and Scherliess*, 1995]. The rapid rise of the F layer over Tirunelveli during the pre-midnight hours clearly indicates the presence of an eastward electric field. The OI 630.0 nm imaging observation over Panhala at these times reveals the presence of broad plasma depletion (reduced airglow intensities appearing as dark bands approximately aligned along the magnetic field (see southwest region of Figure 1i)). The eastward electric field might have provided

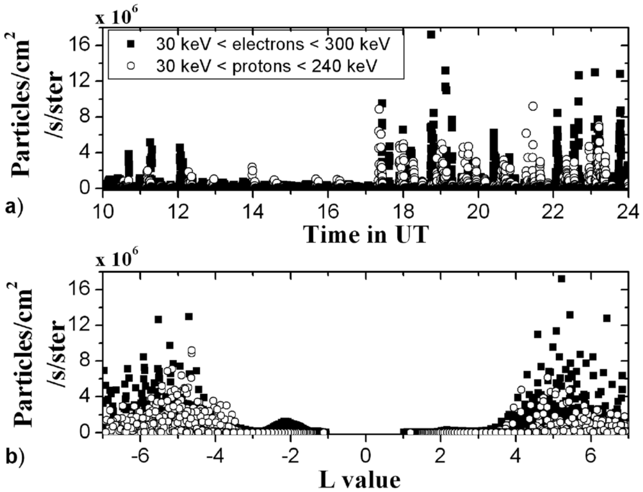

Figure 3. Satellite measurements of precipitating electron and proton fluxes. (a) Time series of fluxes within L value 7 measured by MEPED detector oriented at 90° (see text for details). (b) Measured fluxes with respect to L values (L within 7).

favorable conditions for the fresh generation of *F* region plasma density irregularities near midnight during this disturbed period.

[11] A blanketing sporadic E had occurred over Tirunelveli after local midnight (19:15 UT). Ionospheric sounding records from this site reveal a strong echoing region around 100 km with its characteristic multiple reflections noticed in the ionograms. A sample ionogram recorded at 19:30 UT is shown in Figure 5. The blanketing was so strong that there were no traces of F-layer noticeable in the ionograms. The occurrence of blanketing depends on several factors like wind convergence. But the foremost factor is sufficient production and presence of significant number of electrons at *E* region heights [*Whitehead*, 1966]. Thus, the observed blanketing layer could be taken as an indication for the unusual nighttime ionization in the low latitude Indian sector on the night of streak observations. Earlier theoretical calculations had shown that the ionization created by the energetic particles of ring current origin could account for the enhanced *E* region ionization at low latitudes [*Lyons and Richmond*, 1978; *Tinsley*, 1979].

3. Discussion

[12] Because of the preferred direction of the streaks and they being present in subsequent images at nearly the same location in the sky, the possibility of airplane movements or clouds producing these peculiar filamentary structures was ruled out. They did not appear to arise from any galactic source as their motion was not similar to that of stars. Their origin could not be meteors as there is no reason for the trails of sporadic meteors to maintain a preferred orientation. The meteor trails do get affected by local wave motions and winds at MLT heights that are highly variable both spatially and temporally and hence it is unlikely that the streaks maintained the same directional property as observed here. Moreover, if the streaks were from meteors, they were expected to be observed in other mesospheric emissions as well, especially in sodium images [*Kelley et al.*, 2000; *Kruschwitz et al.*, 2001]. Routine imaging observations have been carried out in the past from several locations even during the period of meteor showers. No earlier imaging observational report from elsewhere resembled the one we are describing here. To our knowledge, no intense meteor showers were reported on the night under consideration. Above all, the visual inspection of the sky during image acquisition did not reveal any clouds or meteors.

[13] The observation site was a hill station without any factories in the immediate neighborhood to release chemical smokes. These signatures do not resemble the typical emissions from powerful rocket launches [*Tagirov et al.*, 2000; *Mendillo et al.*, 2008]. Furthermore, to our knowledge no rocket launches or ionospheric heating experiments were made in the Indian sector around the time of streak observations. Though the spectral distribution of some luminescent flies peak around 550–580 nm [*Seliger et al.*, 1964], it is highly unlikely that they would follow such strict orientation and straight line paths. Further, there was no need for them to always fly to the east of the previous ones. If the features result from the luminescent flies, they are supposed to be present in data during other nights also. Moreover, luminescent flies were not seen over and near the observation site and hence we conclude that the streaks were not because of these flies. Since the possibilities explored above were not likely to be responsible, we anticipate that the reported event was not artificial.

[14] Since the streaks were found only in OI 557.7 nm emission, it is worthwhile to briefly review here the known mechanisms for the generation of this line emission in the Earth's upper atmosphere. This metastable emission is present in both dayglow and nightglow and it results from the transition of $O(^1S)$ to $O(^1D)$ states. The $O(^1D)$ state is another metastable state of atomic oxygen that results in OI 630.0 nm emission while returning to the ground state

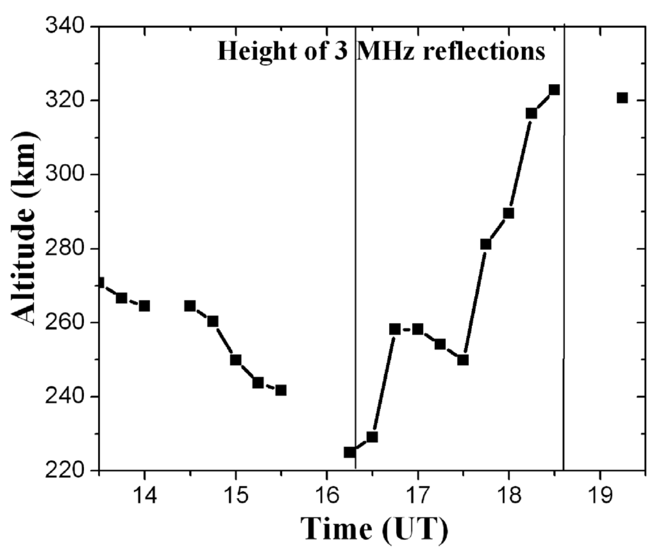

Figure 4. The temporal variation of the base height of the F layer corresponding to the frequency of 3 MHz on the night of 1 February 2008.

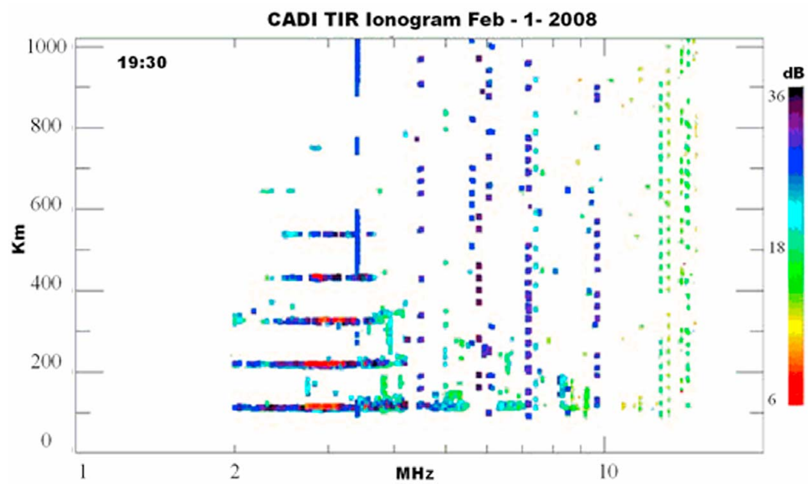

Figure 5. Ionogram recorded at Tirunelveli (8.7°N, 77.8°E geographic; 0.17°S geomagnetic) at 19:30 UT on 1 February 2008.

$O(^3P)$, if not quenched by collisions. The OI 557.7 nm emission is known to arise from a variety of processes like photoelectron impact excitation, photodissociative excitation of molecular oxygen by solar EUV photons, energy transfer from molecular nitrogen to atomic oxygen, dissociative recombination of molecular oxygen ion and three body recombination of atomic oxygen popularly known as Barth Mechanism [*Tyagi and Singh*, 1998, and references cited therein]. These mechanisms are given below in sequence.

$$O + e_{ph} \rightarrow O(^1S) + e_{ph} \quad (1)$$

$$O_2 + h\nu(\lambda < 133.2 \text{ nm}) \rightarrow O + O(^1S) \quad (2)$$

$$N_2^* + O \rightarrow N_2 + O(^1S) \quad (3)$$

$$O_2^+ + e \rightarrow O(^1S) + O \quad (4)$$

$$O + O + M \rightarrow O_2^* + M; O_2^* + O \rightarrow O_2 + O(^1S) \quad (5)$$

Only the last two mechanisms (equations (4) and (5)) contribute to the nightglow. For dayglow, all the five mechanisms are important.

[15] It has been firmly established that the OI 557.7 nm emission always peaks at the lower thermospheric altitude of ~100 km. The life times of $O(^1S)$ and $O(^1D)$ states are 0.91 s and 110 s, respectively. Due to the relatively higher lifetime of $O(^1D)$ state, it is quenched by collisions below ~200 km in the terrestrial atmosphere. The presence of streaks in 557.7 nm emission but not in 630.0 nm emission is a clear indication that the streaks occurred at altitudes below 200 km where the quenching of $O(^1D)$ state prevents OI 630.0 nm emission. Since the peak emission of OI 557.7 nm always occurs at ~100 km, the streaks would have originated at these altitudes. Regular alignment of the observed streaks nearly along the magnetic north-south direction suggests involvement of a charged species in their generation mechanism. This favors the fourth mechanism, namely, the dissociative recombination of molecular oxygen ions and electrons, as the most probable one for the generation of the streaks. At this juncture, it may be noted that the studies of artificial ionospheric heating experiments carried out from Arecibo during the presence of sporadic E layer revealed the occurrence of OI 557.7 nm emission due to the generation of superthermal electrons within the sporadic E plasma clouds [*Kagan et al.*, 2000].

[16] Though we do not have direct observations of energetic neutral atoms (ENA), given the observation of excessive particle fluxes from MEPED instrument and abnormal E region ionization, we first examine the possibility of ENA causing the streaks in OI 557.7 nm emission reported in this work. It is envisaged that energetic secondary electrons produced by the ionization due to the precipitation of ENA got aligned along the magnetic meridian and this might excite ^1S state of oxygen atoms responsible for the greenline emission. The discrete nature of the streaks could be explained if particle precipitation is presumed to occur in patches. Though such a scenario may explain the observed optical phenomenon, their westward tilt and drifts warrant an explanation. Moreover, it is not clear why all newly forming streaks appeared to the east of the existing ones while ENA precipitation will be expected to be diffuse. Further, it is improbable that the secondary electrons produced below 200 km altitudes possessed enough energy to excite several oxygen atoms to ^1S state while retaining their directionality.

[17] Another possibility we examine here is the natural radio wave heating of the ionosphere. In recent years, several studies have been carried out on the induced optical emissions during artificial ionospheric heating experiments with High Frequency (HF) radio waves [*Kagan et al.*, 2000; *Gurevich et al.*, 2002; *Mishin et al.*, 2004; *Pedersen et al.*, 2008]. Especially, *Kagan et al.* [2000] describes observations of OI 557.7 nm emission during high power HF radio heating experiments co-existent with the presence of sporadic E layers. The observations show that the optical emissions maximize in the vicinity of the magnetic zenith. Magnetic

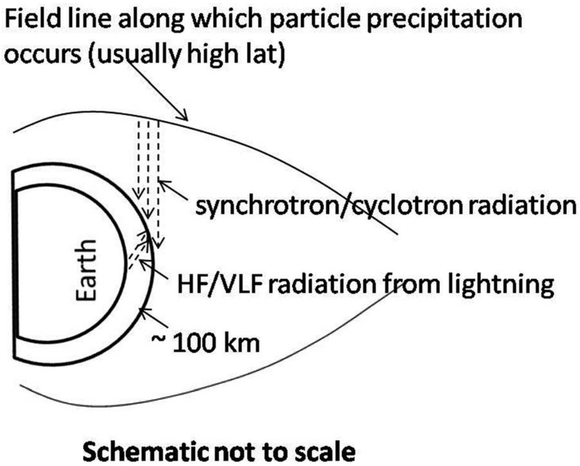

Figure 6. Schematic representation of natural ionospheric heating mechanism proposed herein.

zenith is the point where the line of sight from the transmitter (and hence the radio wave normal) is parallel to the magnetic field. The theories suggested for such emissions rely on different types of plasma resonances to energize the free electrons that result in atomic excitations via collisions.

[18] On the other hand, HF radio noise was observed during aurora and they were attributed to the synchrotron radiation processes [*Dyce and Nakada*, 1959; *Egan and Peterson*, 1960; *Hower and Peterson*, 1964; *Wang et al.*, 1971]. The Auroral Kilometric Radiation (AKR) is a more powerful emission of low frequency radio waves (approximately within 80 to 600 KHz) that was explained elegantly with the help of a cyclotron maser mechanism occurring few thousand kilometers above the auroral zone [*LaBelle and Trueman*, 2006].

[19] Here we suggest that intense HF radio emissions were generated due to increased fluxes of relativistic electrons at very high altitudes in the auroral precipitation zone. As already mentioned, it has been found that the relativistic electron fluxes are more severe in the case of storms generated by CIRs [*Borovsky and Denton*, 2006]. The HF radiation generated at few thousand kilometer altitudes above high latitude region might have reached the *E* region heights above Panhala in an angle possibly attaining magnetic zenith. If the frequency were equal to the upper hybrid frequency (the sum of plasma frequency and electron cyclotron frequency), the HF radiation would energize the plasma by means of resonance instabilities. The nighttime *F* region critical frequency will usually be in the range of 2–4 MHz during solar minimum conditions. From ionograms obtained at Tirunelveli, we noticed unusual nighttime electron concentration (and hence plasma frequency) at *E* region altitudes possibly attributed to particle precipitation. Since the electron cyclotron frequency is relatively large at altitudes below 200 km (~1.2 MHz for a magnetic field of 40000 nT), the upper hybrid frequency at the *E* region heights above Panhala during the observation period would be higher than the penetration frequency of the intervening nighttime F region. In this scenario there was a possibility of natural heating of the E region by means of resonance instabilities, provided the HF radiation of right frequency were generated with sufficient intensity.

[20] At the same time, we cannot rule out the generation of HF emissions from other sources like strong lightning activity in the equatorial zone. Now, transient radio emissions related to lightning activity are well recorded and are known as Trans-Ionospheric Pulse Pairs (TIPPs) and Sub-Ionospheric Pulse Pairs (SIPPs) [e.g., *Massey and Holden*, 1995; *Smith and Holden*, 1996]. The processes related to lightning and its effects on upper atmosphere are only beginning to be understood. It is possible that such lightning induced electromagnetic pulses were responsible for the generation of superthermal electrons at *E* region heights that are capable of exciting O atoms to ^1S state, resulting in the observed emissions. We have focused our discussion mainly on the natural heating of ionosphere by HF radiation owing to the similarities of the current event with few observations of artificial aurora generated by ionospheric modification experiments [*Kagan et al.*, 2000].

[21] In the past, heating of lower ionosphere by VLF waves and associated excitation of atoms resulting in transient luminous events (TLEs) have been well recorded [*Inan et al.*, 1991; *Fukunishi et al.*, 1996]. It is not known whether such waves contribute to the heating of the ionosphere and subsequent generation of the streaks observed in this work. Though the VLF heating, which is common during intense thunderstorms, could be a potential mechanism for triggering such streaks, we still need to explain the rarity of the current observations.

[22] If such radio emissions from lightning sources were responsible for the streaks in 557.7 nm airglow, then the orientation of the streaks can be explained by the location of the sources. Interestingly, to the southeast of the observation site, intense convection-prone region of maritime continent (Indonesian region) is situated. In Figure 6 we show a tentative schematic of the natural radio wave heating mechanism speculated in this work. Unfortunately, we lack data on lightning in and around Indian sector during the observation period to probe its efficacy further.

4. Summary

[23] The present work documents an unusual imaging observation of filamentary structures in OI 557.7 nm emission (not in other emissions) during a moderate geomagnetic storm triggered by a CIR. Observations suggest the presence of prompt penetration eastward disturbance electric field in the low latitude Indian sector and increase in ring current particle precipitation. Unusual enhancement in nighttime ionization (inferred from blanketing layer over equator) was also noticed. In this work we examined a few mechanisms. One of them is purely based on ENA precipitation. Other mechanisms are based on the idea of natural radio wave heating of the ionosphere. Radio waves responsible for this phenomenon are speculated to arise in either high latitude synchrotron radiation or lightning induced electromagnetic pulses. The mechanisms based on radio wave heating of the ionosphere appear to be more probable. However, they need to be substantiated or discredited by theoretical calculations and further observations. If lightning induced radio waves are found to be responsible for such emissions, observations

and analysis of the events of this kind would give rise to new insights into the atmosphere-ionosphere coupling.

[24] **Acknowledgments.** This work was supported by the Department of Science and Technology, government of India. We acknowledge NGDC data center and the team members of NOAA/POES satellite mission for providing valuable data. One of the authors (V.L.N.) thanks the director, Indian Institute of Geomagnetism, for a research scholarship.

[25] Robert Lysak thanks Shoichi Okano and the other reviewers for their assistance in evaluating this paper.

References

Abalde, J. R., P. R. Fagundes, J. A. Bittencourt, and Y. Sahai (2001), Observations of equatorial F region plasma bubbles using simultaneous 777.4 nm and 630.0 nm imaging: New results, *J. Geophys. Res.*, *106*, 30,331–30,336, doi:10.1029/2001JA001115.

Baker, D. N., J. B. Blake, D. J. Gorney, P. R. Higbie, R. W. Klebesadel, and J. H. King (1987), Highly relativistic magnetospheric electrons: A role in coupling to the middle atmosphere?, *Geophys. Res. Lett.*, *14*, 1027–1030, doi:10.1029/GL014i010p01027.

Bernhardt, P. A., C. A. Tepley, and L. M. Duncan (1988), Artificial airglow excited by high power radio waves, *Science*, *242*, 1022–1027, doi:10.1126/science.242.4881.1022.

Borovsky, J. E., and M. H. Denton (2006), Differences between CME-driven storms and CIR-driven storms, *J. Geophys. Res.*, *111*, A07S08, doi:10.1029/2005JA011447.

Chapman, S. (1957), The aurora in middle and low latitudes, *Nature*, *179*, 7–11, doi:10.1038/179007a0.

Dyce, R. B., and M. P. Nakada (1959), On the possibility of detecting synchrotron radiation from electrons in the Van Allen belts, *J. Geophys. Res.*, *64*, 1163–1168, doi:10.1029/JZ064i009p01163.

Egan, R. D., and A. M. Peterson (1960), Auroral noise at HF, *J. Geophys. Res.*, *65*, 3830–3832, doi:10.1029/JZ065i011p03830.

Fejer, B. G., and L. Scherliess (1995), Time-dependent response of equatorial ionospheric electric fields to magnetospheric disturbances, *Geophys. Res. Lett.*, *22*, 851–854, doi:10.1029/95GL00390.

Fukunishi, H., Y. Takahashi, M. Kubota, K. Sakonai, U. S. Inan, and W. A. Lyons (1996), Elves: Lightning-induced transient luminous events in the lower ionosphere, *Geophys. Res. Lett.*, *23*, 2157–2160, doi:10.1029/96GL01979.

Gurevich, A. V., K. P. Zybin, H. C. Carlson, and T. Pedersen (2002), Magnetic zenith effect in ionospheric modifications, *Phys. Lett. A*, *305*, 264–274, doi:10.1016/S0375-9601(02)01450-0.

Hower, G. L., and A. M. Peterson (1964), Synchrotron radiation from auroral electrons, *J. Geophys. Res.*, *69*, 3995–4001, doi:10.1029/JZ069i019p03995.

Inan, U. S., T. F. Bell, and J. V. Rodriguez (1991), Heating and ionization of the lower ionosphere by lightning, *Geophys. Res. Lett.*, *18*, 705–708, doi:10.1029/91GL00364.

Kagan, L. M., M. C. Kelley, F. Garcia, P. A. Bernhardt, F. T. Djuth, M. P. Sulzer, and C. A. Tapley (2000), The structure of electromagnetic wave-induced 557.7-nm emission associated with a sporadic E event over Arecibo, *Phys. Rev. Lett.*, *85*, 218–221, doi:10.1103/PhysRevLett.85.218.

Kagan, L. M., J. W. MacDougall, and M. C. Kelley (2009), A mechanism for extraordinary bright radiowave-induced aurora in the ionospheric E region, *J. Atmos. Sol. Terr. Phys.*, *71*, 553–558, doi:10.1016/j.jastp.2009.01.006.

Kelley, M. C., et al. (2000), First observation of long lived meteor trains with resonance lidar and other optical instruments, *Geophys. Res. Lett.*, *27*, 1811–1814, doi:10.1029/1999GL011175.

Kruschwitz, C. A., et al. (2001), Observations of persistent Leonid meteor trails: 2. Photometry and numerical modeling, *J. Geophys. Res.*, *106*, 21,525–21,541, doi:10.1029/2000JA000174.

LaBelle, J. W., and R. A. Trueman (2006), Geospace electromagnetic waves and radiation, *Lect. Notes Phys.*, *687*, Springer, Berlin, doi:10.1007/b11580119.

Lyons, L. R., and A. D. Richmond (1978), Low latitude E region ionization by energetic ring current particles, *J. Geophys. Res.*, *83*, 2201–2204, doi:10.1029/JA083iA05p02201.

Massey, R. S., and D. N. Holden (1995), Phenomenology of transionospheric pulse pairs, *Radio Sci.*, *30*, 1645–1659, doi:10.1029/95RS01563.

Mendillo, M., S. Smith, A. Coster, P. Erickson, J. Baumgardner, and C. Martinis (2008), Man-made space weather, *Space Weather*, *6*, S09001, doi:10.1029/2008SW000406.

Mishin, E. V., W. J. Burke, and T. Pedersen (2004), On the onset of HF-induced airglow at HAARP, *J. Geophys. Res.*, *109*, A02305, doi:10.1029/2003JA010205.

Narayanan, V. L., S. Gurubaran, and K. Emperumal (2009), Imaging observations of upper mesospheric nightglow emissions from Tirunelveli (8.7°N), *Indian J. Radio Space Phys.*, *38*, 150–158.

Narayanan, V. L., S. Gurubaran, and K. Emperumal (2010), Airglow imaging observations of small-scale structures driven by convective instability in the upper mesosphere over Tirunelveli (8.7°N), *J. Geophys. Res.*, *115*, D19119, doi:10.1029/2009JD012937.

Pedersen, T., R. Esposito, E. Kendall, D. Sentman, M. Kosch, E. Mishin, and R. Marshall (2008), Observations of artificial and natural optical emissions at the HAARP facility, *Ann. Geophys.*, *26*, 1089–1099, doi:10.5194/angeo-26-1089-2008.

Seliger, H. H., J. B. Buck, W. G. Fastie, and W. D. McElroy (1964), The spectral distribution of firefly light, *J. Gen. Physiol.*, *48*, 95–104, doi:10.1085/jgp.48.1.95.

Shiokawa, K., Y. Otsuka, T. Ogawa, N. Balan, K. Igarashi, A. J. Ridley, D. J. Knipp, A. Saito, and K. Yumoto (2002), A large-scale traveling ionospheric disturbance during the magnetic storm of 15 September 1999, *J. Geophys. Res.*, *107*(A6), 1088, doi:10.1029/2001JA000245.

Shiokawa, K., T. Ogawa, and Y. Kamide (2005), Low-latitude auroras observed in Japan: 1999–2004, *J. Geophys. Res.*, *110*, A05202, doi:10.1029/2004JA010706.

Silverman, S. M. (2003), Sporadic auroras, *J. Geophys. Res.*, *108*(A4), 8011, doi:10.1029/2002JA009335.

Smith, D. A., and D. N. Holden (1996), Ground-based observations of subionospheric pulse pairs, *Radio Sci.*, *31*, 553–571, doi:10.1029/96RS00007.

Tagirov, V. R., V. A. Arinin, V. V. Klimenko, A. Pajunpaa, and U. Brandstorm (2000), Optical phenomena in the atmosphere caused by powerful rocket launches, *Phys. Chem. Earth*, *25*, 551–558.

Taylor, M. J., M. B. Bishop, and V. Taylor (1995), All-sky measurements of short period waves imaged in OI(557.7nm), Na(589.2nm) and near infrared OH and $O_2(0,1)$ nightglow emissions during the ALOHA-93 campaign, *Geophys. Res. Lett.*, *22*, 2833–2836, doi:10.1029/95GL02946.

Tinsley, B. A. (1979), Energetic neutral atom precipitation during magnetic storms: Optical emission, ionization, and energy deposition at low and middle latitudes, *J. Geophys. Res.*, *84*, 1855–1864, doi:10.1029/JA084iA05p01855.

Tinsley, B. A., R. P. Rohrbaugh, H. Rassoul, E. S. Barker, A. L. Cochran, W. D. Cochran, B. J. Willis, D. W. Willis, and D. Slater (1984), Spectral characteristics of two types of low latitude aurorae, *Geophys. Res. Lett.*, *11*, 572–575, doi:10.1029/GL011i006p00572.

Tinsley, B. A., R. Rohrbaugh, H. Rassoul, Y. Sahai, N. R. Teixeira, and D. Slater (1986), Low latitude aurorae and storm time current systems, *J. Geophys. Res.*, *91*, 11,257–11,269, doi:10.1029/JA091iA10p11257.

Tyagi, S., and V. Singh (1998), The morphology of oxygen greenline dayglow emission, *Ann. Geophys.*, *16*, 1599–1606, doi:10.1007/s00585-998-1599-z.

Wang, C. S., Y. H. Lee, and J. S. Kim (1971), Synchrotron radiation from auroral electrons, *Radio Sci.*, *6*, 775–780, doi:10.1029/RS006i008p00775.

Whitehead, J. D. (1966), Mixtures of ions in the wind-shear theory of sporadic E, *Radio Sci.*, *2*, 198–203.

Willis, D. M., F. R. Stephenson, and H. Fang (2007), Sporadic aurorae observed in East Asia, *Ann. Geophys.*, *25*, 417–436, doi:10.5194/angeo-25-417-2007.

K. Emperumal, S. Gurubaran, and V. L. Narayanan, Equatorial Geophysical Research Laboratory, Indian Institute of Geomagnetism, Tirunelveli 627 011, India. (narayananvlwins@gmail.com)

P. T. Patil, Radar Observatory, Indian Institute of Geomagnetism, Shivaji University Campus, Kolhapur 416 004, India.